March 15, 2002

Effect of Ni on the transport and magnetic properties of Co1ÀxNixSb3

Jeffrey Dyck, *John Carroll University*
Wei Chen
Jihui Yang
Gregory P. Meisner
Ctirad Uher

Effect of Ni on the transport and magnetic properties of $Co_{1-x}Ni_xSb_3$

Jeffrey S. Dyck,[1] Wei Chen,[1] Jihui Yang,[2] Gregory P. Meisner,[2] and Ctirad Uher[1]
[1]*Department of Physics, University of Michigan, Ann Arbor, Michigan 48109*
[2]*Materials and Processes Laboratory, GMR&D Center, Warren, Michigan 48090*
(Received 1 June 2001; revised manuscript received 9 October 2001; published 15 February 2002)

The filled skutterudite compounds based on the binary skutterudite $CoSb_3$ are currently being investigated for their potential applications as thermoelectric materials. One route to optimization of these compounds is by doping on the Co site. An obvious candidate for an *n*-type dopant is Ni, since it has one more electron in its valence shell than Co. Up to now, however, only high concentrations of Ni in $CoSb_3$ have been studied; and the valence of Ni in this compound and its influence on the transport and magnetic properties has been an open question. We present electrical resistivity, thermopower, Hall effect, magnetoresistance, and magnetic susceptibility measurements on polycrystalline, *n*-type $Co_{1-x}Ni_xSb_3$ with $x=0$, 0.001, 0.003, 0.005, 0.0075, and 0.01. Our results show that in these low concentrations Ni has a dramatic effect on the transport properties. A two-band model is proposed that takes into account transport in both the conduction band and within donor impurity states formed by the Ni impurities. This model provides a consistent explanation of both the anomalous low-temperature transport properties as well as the Curie-Weiss behavior of the magnetic susceptibility. We conclude that Ni takes the tetravalent Ni^{4+} state, assumes the d^6 electronic configuration for the lower energy nonbonding orbitals, and gives an electron to the conduction band.

DOI: 10.1103/PhysRevB.65.115204 PACS number(s): 71.55.Ht, 72.20.Pa, 72.20.Ee, 75.50.Pp

I. INTRODUCTION

Skutterudites have received considerable attention over the past several years as prospective novel thermoelectric materials.[1,2] The skutterudite structure, designated as MX_3 ($M=$Co, Rh, or Ir and $X=$P, As, or Sb), is characterized by two large voids (or cages) within the unit cell that can accommodate certain rare-earth elements,[3] alkaline earths,[4] or even monovalent thallium.[5] In the filled skutterudites, the filler atom R supplies extra electrons to the structure, so the appropriate chemical formula is RT_4X_{12}, where T represents a transition metal with one less electron than M thereby stabilizing the structure. Filled skutterudites have much lower thermal conductivities than their binary counterparts because the guest atoms "rattle" inside these oversized cages, disrupting phonon transport. In the case of $Ce_yFe_{4-x}Co_xSb_{12}$, Meisner *et al.*[6] found that a fractionally filled (near 50% void occupancy) composition minimized the thermal conductivity. Fe must be added to this compound in order to accommodate Ce, though its exact role in the characteristics of the material has been a puzzle (see, for example, Ref. 7). Further optimization of the thermoelectric properties of materials like this one takes place via doping. Therefore, both *p*-type (e.g., Fe on the Co site or Sn on the Sb site) as well as *n*-type dopants must be identified and studied.

The skutterudites that have attracted by far the greatest attention are compounds based on $CoSb_3$. They show not only some of the best thermoelectric characteristics, but the constituent elements are also abundant, less volatile, and markedly less expensive than most of the alternative skutterudite structures. $CoSb_3$ is a small gap semiconductor, and transport properties of this material (single crystals as well as polycrystalline specimens) have been studied extensively.[8–13] Some forty years ago, Dudkin and his colleagues[14,15] established that one could substitute on both the transition-metal site and on the pnicogen lattice. We, along with others,[7,16–18] have shown that replacing a small fraction of Co atoms with Fe has a remarkably strong influence on the nature of the charge-carrier transport and on the propagation of phonons. Anno *et al.*[19] have published recently an interesting study that indicated a strong influence of Ni on the electronic properties of $CoSb_3$. In their work they used Ni concentrations above 3 at.%, a rather high level of substitution that resulted in 2–3 orders of magnitude higher free carrier concentration than that observed in pure $CoSb_3$. We were interested in exploring the influence of much lower doping levels of Ni, and in this paper we present our findings on the influence of Ni at concentrations below 1 at.%.

At the heart of the issue of Ni-doped $CoSb_3$ is the valence state of Ni. Previous magnetic studies[20] have suggested Ni is in the low-spin ($s=1/2$) $3d^7$ configuration because of a Curie-Weiss-like paramagnetic susceptibility; yet the carrier concentration increases with Ni doping, which implies that Ni takes a $3d^6$ electronic configuration and should have zero spin. In the course of our study, we discovered that very low doping levels of Ni have a spectacular effect on the transport behavior of the compound, especially at low temperature, leading us to believe two conduction channels were necessary to explain the behavior. A straightforward look at the impurity states associated with the conduction band in $CoSb_3$ shows a small ground-state Bohr radius because of the very high dielectric constant and large electron effective mass. As a result, impurity transport effects can reveal themselves up to relatively high impurity concentrations. In this paper, we present a model that takes into account transport in both the conduction band and within donor impurity states formed by the Ni impurities. This two-band model can explain *both* the transport and magnetic properties of $Co_{1-x}Ni_xSb_3$.

II. SAMPLES AND EXPERIMENTAL TECHNIQUE

Polycrystalline $CoSb_3$ and its Ni-doped forms were prepared from high purity starting materials (99.995% purity for

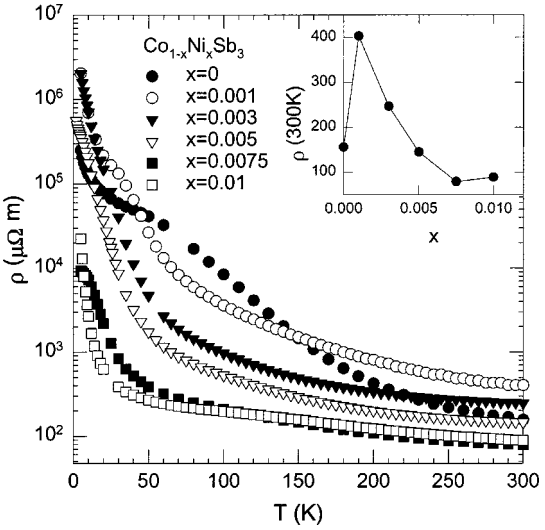

FIG. 1. Electrical resistivity ρ of $Co_{1-x}Ni_xSb_3$ versus temperature. The inset is a plot of resistivity at 300 K versus Ni concentration x.

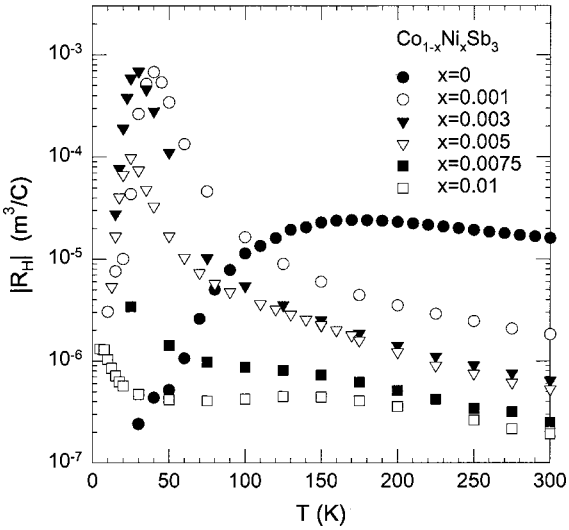

FIG. 2. Hall coefficient R_H for $Co_{1-x}Ni_xSb_3$ versus temperature. For $x=0$, R_H is positive; for $x\neq 0$, R_H is negative.

Co, 99.999% purity for Sb, and 99.999% purity for Ni) by induction melting the constituents at 1400 °C for a brief period of time, followed by annealing at 700 °C under argon for 20 h. Sample stoichiometry is checked by electron-probe microanalysis. The skutterudite phase is confirmed by x-ray power diffraction. Moreover, there is no secondary phase, which is further confirmed by electron-probe microanalysis. All samples are very close to stoichiometry. Electron backscatter imaging and optical microscopy revealed an average grain size of 10 μm. Samples are cut from the ingots with typical dimensions $3\times3\times8$ mm^3.

Galvanomagnetic measurements are performed using a 16 Hz Linear Research bridge in conjunction with a cryostat equipped with a 5 T superconducting magnet. Hall effect studies are done in both positive and negative magnetic field to correct for any misalignment of the Hall probes. Thermal-transport studies are made with the aid of a longitudinal steady-state technique in the range 2–300 K. We use copper-constantan thermocouples made from very thin wires (25 μm diameter) to measure a thermal gradient set up by a small strain gauge heater attached to a free end of the sample. The copper legs of the thermocouple serve as voltage probes for thermopower measurements. Correction for the thermopower of the copper legs is based on independent measurements of their thermopower against a high-T_c sample and against a Pb standard.[21] Magnetization measurements are done in a quantum-design magnetometer between 10–300 K in applied magnetic fields up to 5 T. For each sample the background magnetic moment of the plastic sample container was subtracted from the measured magnetic moment at each temperature and at each magnetic field.

III. RESULTS

In Fig. 1, we plot the temperature dependence of the electrical resistivity. At room temperature, the resistivity first increases with the addition of Ni, reflecting the change from the high-mobility p-type to low-mobility n-type conduction. Further increase of the Ni concentration results in a reduction of ρ(300 K) up to $x=0.0075$ where it begins to increase slightly. Over the entire temperature range all samples display an activated behavior. While the low-temperature semiconducting behavior has been seen before,[11,13] the increase in resistivity over several orders of magnitude below about 50 to 100 K is a testament to the high purity and crystalline quality of the samples; therefore, the possibility of gleaning information from low-temperature transport measurements is promising.

The Hall coefficient R_H as a function of temperature is shown in Fig. 2. It should be noted that R_H showed some variation with magnetic-field strength at lower temperatures that suggests the participation of charge carriers from more than one energy band. As $CoSb_3$ is a narrow-gap semiconductor, the energy bands are expected to display a nonparabolic dispersion for moderate carrier concentrations. However, as others have done,[1] we estimate the carrier concentration assuming a parabolic band at room temperature using $p,n=\pm 1/(R_He)$ where e is the charge of the carrier. The pure $CoSb_3$ has a room-temperature hole concentration of 3.7×10^{17} cm^{-3} which is low compared to that for other polycrystalline $CoSb_3$.[13,18,22] Rather, this carrier concentration is typical of that for single crystal $CoSb_3$[8,11,12] and this indicates very good stoichiometry. All of the Ni-doped samples had negative R_H, indicating dominant n-type conduction. Figure 3 plots the room-temperature carrier concentration in relation to Ni concentration. One can see that the data fall on a straight line, except for the 0.5% Ni sample. Therefore, a clear doping effect is apparent and is consistent with Ni substituting for Co in the skutterudite lattice and donating its extra electron to the conduction band. However, at this temperature, the efficiency of the ionization is only 30%. The most striking feature in the Hall data is the sharp peak at low temperatures that moves to lower temperatures as the Ni concentration is increased. A similar effect was also seen in the magnetoresistance (see below).

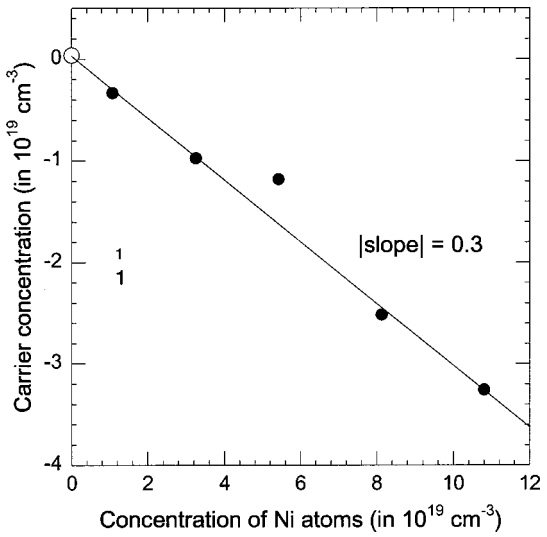

FIG. 3. Room-temperature carrier concentration for $Co_{1-x}Ni_xSb_3$ as a function of Ni concentration. The open circle represents data for the *p*-type pure $CoSb_3$ sample. The line is a guide for the eye.

Figure 4 shows the temperature dependence of the Hall mobility, $\mu_H = R_H/\rho$, for all of the samples. At room temperature, μ_H of $CoSb_3$ is approximately 1250 cm^2/V s, which compares well to previous reports[13] for polycrystalline material but is 2–3 times lower than that for single crystals.[8,10,11] For Ni-doped samples, $\mu_H = 45$ cm^2/V s for 0.1% Ni and decreases to 22 cm^2/V s for 1% Ni. These values, as well as carrier concentration dependence, are the same as that seen by Anno[19] for Ni-doped $CoSb_3$ if one makes an extrapolation to the lower carrier concentrations considered here. The Hall mobility of *n*-type samples follows

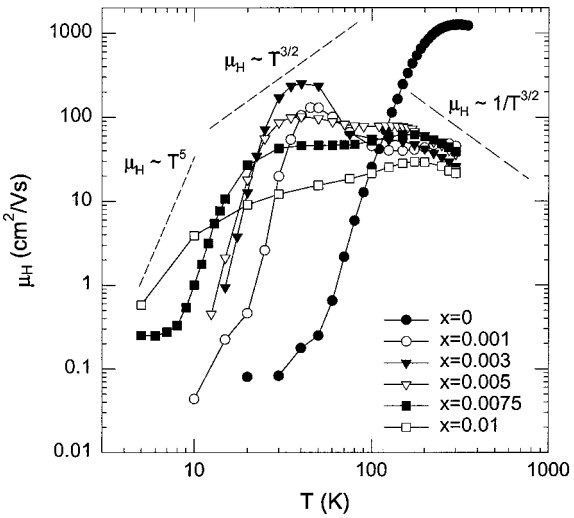

FIG. 4. Temperature dependence of the Hall mobility μ_H for $Co_{1-x}Ni_xSb_3$. The dependences expected from scattering due to ionized impurities ($T^{3/2}$) and acoustic phonons ($1/T^{3/2}$) are indicated by dashed lines. The sharp decrease with temperature at the lowest temperatures indicates a breakdown of the single-carrier picture. A T^5 dependence is also shown to highlight the strong temperature dependence.

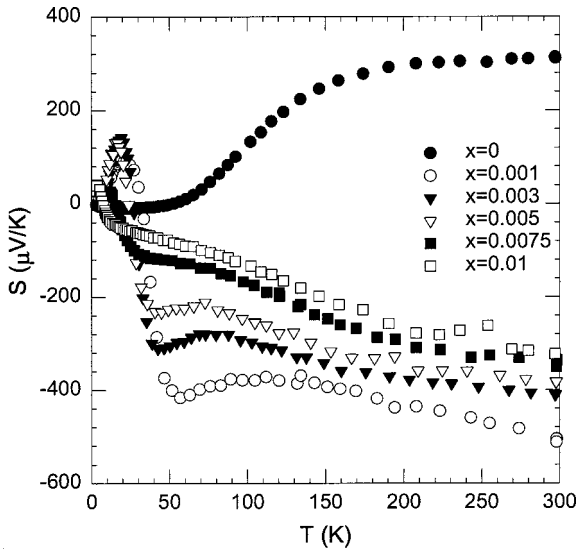

FIG. 5. Temperature dependence of the thermopower *S* for $Co_{1-x}Ni_xSb_3$.

roughly a $1/T^{3/2}$ dependence near room temperature indicative of acoustic phonon scattering; however, the dependence is shallower for the undoped sample, which suggests that scattering due to impurities is also present. Below about 150 K, the slope of the curve is much steeper than a $T^{3/2}$ dependence that would be expected from ionized impurity scattering. In fact, for most of the samples, the slope approaches T^5. As the Ni content increases, the onset of a sharp decrease in mobility occurs at lower temperatures, and finally is not observed at all for $x = 0.01$. We rule out grain boundary scattering as being responsible for this effect because the temperature dependence does not follow the known relation $\mu_H \propto T^{-1/2} \exp[-E_B/k_BT]$ where E_B is the energy barrier at grain boundaries.[23]

In Fig. 5 we show the temperature dependence of the thermopower *S* for $Co_{1-x}Ni_xSb_3$. Pure $CoSb_3$ is *p*-type and has positive room temperature thermopower. Ni concentrations of only 0.1% drastically affect this picture, changing the sign and showing the largest magnitude of approximately -500 μV/K. Further addition of Ni increases the carrier concentration and, therefore, decreases the magnitude of *S* at room temperature. The most interesting aspect of these data is the dramatic low-temperature anomaly where the sign of *S* is opposite to that of R_H. We reject phonon drag as an explanation of this anomaly as it is absent in the $x = 0$ sample. For all of the Ni-doped $CoSb_3$ samples, the temperature dependence of the peak positions in the Hall coefficient follow a similar trend as the thermopower.

From the temperature dependence of μ_H we have determined that the dominant carrier scattering mechanism at room temperature for Ni-containing samples is acoustic phonon scattering. Then, assuming a single parabolic band, we calculated the reduced Fermi energy η from the experimental thermopower data using[24]

$$S = -\frac{k_B}{e}\left[\frac{2F_1(\eta)}{F_0(\eta)} - \eta\right], \tag{1}$$

where k_B is Boltzmann's constant, e is the charge of the electron, and F_x is a Fermi integral of order x. Using the calculated η, the carrier concentration n can be expressed as

$$n = 4\pi\left(\frac{2m_n k_B T}{h^2}\right)^{3/2} F_{1/2}(\eta), \tag{2}$$

where m_n is the effective mass, T is the temperature, and h is Planck's constant. The effective masses as a function of Ni concentration were calculated and had values between $3m_0$ and $4m_0$, where m_0 is the free electron mass—no clear trend was evident. Upon analysis of the temperature dependence of the Hall mobility for the pure $CoSb_3$, we note that the scattering mechanism is of a somewhat mixed nature, though primarily due to acoustical phonons yielding a hole effective mass of $0.175m_0$.

Considering the fact that S becomes opposite in sign to R_H and the Hall mobility has an unusually sharp drop at low temperatures, we conclude that a second conduction channel is necessary to explain the behavior. Several researchers have indicated that impurity band conduction may become an issue for nominally undoped, p-type $CoSb_3$.[11–13] We show that our data for lightly n-type $Co_{1-x}Ni_xSb_3$ are also consistent with the onset of impurity conduction at low temperatures and the effect is much greater than what was expected. In the discussion below, we attempt to interpret the data with this in mind, and extend the analysis to better understand the striking features in the low-temperature transport for p-type and, particularly, n-type samples. Then, we introduce and discuss the magnetic susceptibility results.

IV. DISCUSSION

A. Nominally undoped p-type $CoSb_3$

In Fig. 6(a), we show a plot of $\log(\rho)$ and $\log(R_H)$ as a function of inverse temperature for the nominally undoped $CoSb_3$. The resistivity profile is very similar to those reported by several researchers.[11–13] The high-temperature region can be described by the equation $\rho = \rho_0 \exp[E_a/(k_B T)]$ (shown by the solid line), where the activation energy, $E_a = 51$ meV and k_B is Boltzmann's constant. This activation energy could imply an intrinsic semiconducting energy gap of ~102 meV. This result is in good agreement with previous experiments and calculations.[11,25,26] R_H has a maximum with approximately exponential temperature dependence on both sides of the peak that is a characteristic sign of the low-temperature onset of transport in a band formed by shallow impurity levels.

Arushanov *et al.*[12] described a very similar temperature dependence of the Hall coefficient in lightly doped $CoSb_3$ single crystals by assuming the existence of an acceptor impurity band. However, an additional deep acceptor level was needed to account for the behavior because the value of the activation energy estimated on the basis of the high-temperature data (higher than R_{max}) was more than an order of magnitude larger than the value derived from the low-temperature region (lower than R_{max}). They reported $N_{A1} = 1.5–3\times10^{17}$ cm^{-3} and $N_{A2} = 1.2–1.4\times10^{17}$ cm^{-3} for the concentration of shallow and deep acceptors, respectively;

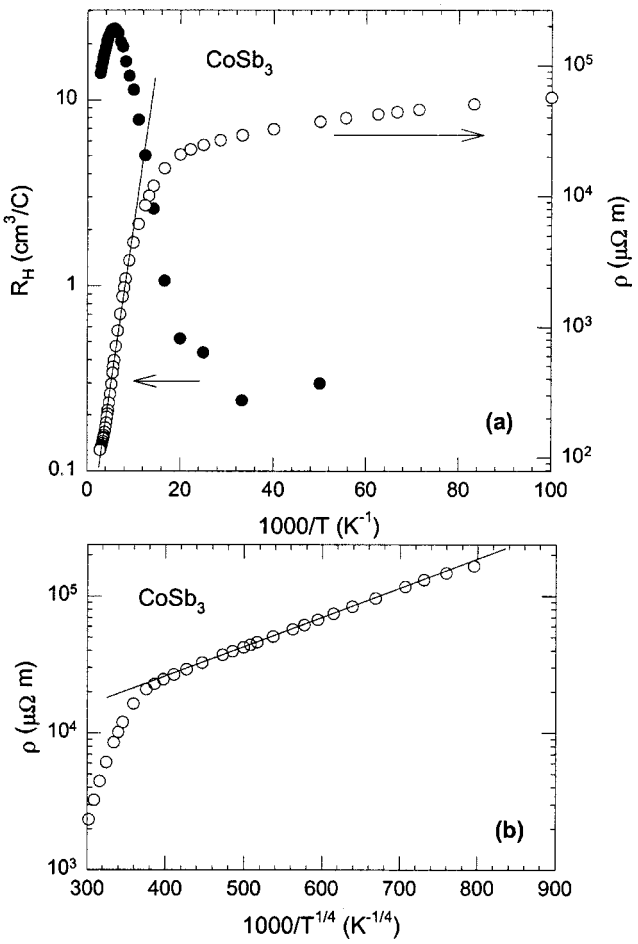

FIG. 6. (a) Hall coefficient R_H and resistivity ρ versus temperature for $CoSb_3$. The solid line indicates $\rho(T) = \rho_0 \exp[(E_a/k_B T)]$ with $E_a = 51$ meV for $T \geq 125$ K. (b) Low temperature resistivity characterized by $\rho(T) = \rho_0 \exp[(T_0/T)^{1/4}]$ with $T_0 = 584$ K (solid line), for $T \leq 30$ K.

$N_d = 0.9–1.6\times10^{17}$ cm^{-3} for the concentration of compensating donor levels; and $E_{A1} < 1$ meV and $E_{A2} = 38–47$ meV for the activation energies of the shallow and deep acceptor levels, respectively. Our data can also be described using the same model as in Ref. 12, but with only one acceptor level since the activation energies on either side of R_{max} are approximately the same. We obtain a concentration of acceptor levels $N_a = 1.4\times10^{18}$ cm^{-3} with activation $E_a = 31.5$ meV and a concentration of compensating donors $N_d = 2.7\times10^{17}$ cm^{-3}.

Below 30 K, ρ has a *nearly* exponential temperature dependence with much lower activation energy, and clearly much lower mobility as indicated by Fig. 4. The best fit [see Fig. 6(b)] to the data in this temperature region was of the form,

$$\rho(T) = \rho_0 \exp\left[\left(\frac{T_0}{T}\right)^{1/4}\right], \tag{3}$$

where ρ_0 is a material constant and T_0 is the characteristic temperature of the system. Within a model of impurity conduction, this behavior could be indicative of Mott variable

range hopping (VRH).[27] This fit was substantially better than if in Eq. (3) an exponent of $\frac{1}{2}$ was used instead of $\frac{1}{4}$, suggesting there is no Coulomb gap. We cannot strictly exclude other low-mobility transport mechanisms (e.g., small polaron) to account for this low-temperature behavior, but we pursue hopping transport as a likely scenario given the prior works suggesting impurity-transport effects at low temperature. The characteristic temperature is expressed as[27]

$$T_0=\frac{\beta\alpha^3}{k_B g_f}, \tag{4}$$

where α^{-1} is the localization length of the impurity wave function, g_f is the density of states at the Fermi level, and β is a constant. Furthermore, we take

$$g_f=\frac{N_a}{w}, \tag{5a}$$

$$w=\frac{e^2}{\varepsilon_0 r}, \tag{5b}$$

$$r=\left(\frac{3}{4\pi N_a}\right)^{1/3}, \tag{5c}$$

where w is the impurity bandwidth (approximated by the magnitude of the Coulomb interaction) and r is the distance between impurities. Assuming α^{-1} to be the Bohr radius, $a_B=\varepsilon_0/(m_p/m_0)0.52$ Å, of the ground state of the doping impurity in a hydrogenic model, α^{-1} is calculated to be approximately 100 Å (assuming $\varepsilon_0=33.5$ (Ref. 28) and $m_p=0.175m_0$). From the fit it was found that $T_0=584$ K, which yields $N_a=6\times10^{17}$ cm^{-3} if one takes $\beta=5.7$.[27] This value is consistent with the estimate of N_a from the Hall analysis above. VRH is expected in impurity semiconductors at low temperatures when $w/k_BT\sim2\alpha r$. This condition is satisfied at these temperatures assuming the above parameters.

B. Ni-doped $CoSb_3$

In Fig. 7, we plot log(ρ) versus inverse temperature for $Co_{0.997}Ni_{0.003}Sb_3$. All of the resistivity curves have very similar temperature dependences and are well described by the equation

$$\rho(T)=\rho_0\exp\left(\frac{\varepsilon_0}{k_BT}\right)+\rho_1\exp\left(\frac{\varepsilon_1}{k_BT}\right)+\rho_3\exp\left(\frac{\varepsilon_3(T)}{k_BT}\right), \tag{6}$$

with the activation energies $\varepsilon_0>\varepsilon_1>\varepsilon_3$. For increasing Ni concentration, these energy levels decrease, shifting the "knee" between the middle and lower temperature regimes to lower temperature. When compared to Hall data, it is seen that the peak in R_H occurs at the temperature of the crossover between the middle (ε_1) and lower (ε_3) activation regions. From this observation we infer that the ε_1 level is associated with a donor impurity and ε_3 relates to hopping within the impurity "band." The ε_0 level is likely due to the intrinsic band gap, but could arise from a deeper donor level—we do not extend the data to high-enough temperatures to get an accurate estimate of this energy level. ε_3 is temperature dependent at very low temperatures, though a distinct value of ε_3 is observed over an extended temperature for $x<0.0075$. Below about 5 K, the resistivities of all of the samples again fit Eq. (3) (see inset to Fig. 7), which is suggestive of VRH of carriers among the impurity states. Quantitative analysis of this behavior is not warranted given the relatively narrow temperature range over which it is observed.

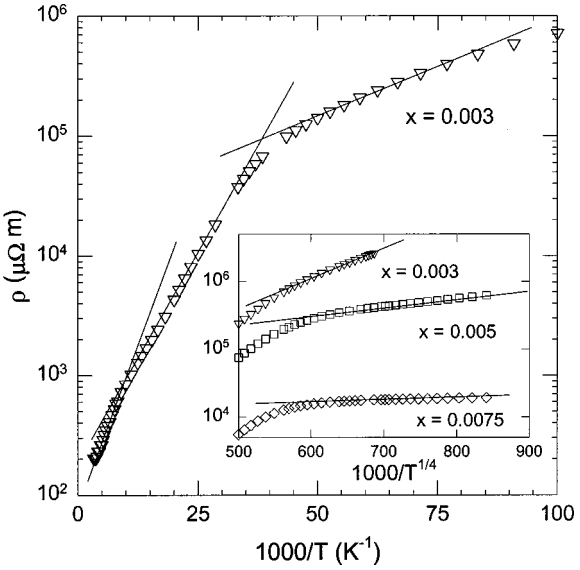

FIG. 7. log(ρ) versus inverse temperature for $Co_{0.997}Ni_{0.003}Sb_3$. The straight lines highlight regions of activated temperature dependence. The inset indicates the low-temperature ρ data behaves according to Eq. (3).

Given the evidence for transport of electrons both in the conduction band and among impurities, we analyze the transport properties in terms of a simple, two-band model described by n_c, μ_c, σ_c, n_i, μ_i, and σ_i that are the electron concentration, mobility, and conductivity in the conduction band and impurity states, respectively. The goal of this analysis is to elucidate the physical mechanism responsible for anomalous transport in $Co_{1-x}Ni_xSb_3$ with $x<0.01$. As such, we focus on the low-temperature region near the peak in R_H and the change of sign of S. These anomalous transport features presumably exist at temperatures lower than those explored for $Co_{0.99}Ni_{0.01}Sb_3$; therefore, we do not include this sample in the analysis. Within the framework of semiconductor statistics and taking into account one donor level and one compensating acceptor level, which is appropriate below 100 K,

$$n_c+N_a=\frac{N_d}{1+\dfrac{\gamma n_c}{N_c}\exp\left(\dfrac{E_d}{k_BT}\right)}. \tag{7}$$

Here, $N_c=2(m_nk_BT/2\pi\hbar^2)^{3/2}$ is the density of states in the conduction band, N_a is the concentration of compensating acceptors, and the degeneracy factor γ is taken to be 6. Sofo and Mahan have calculated the electronic band structure of $CoSb_3$ and concluded that the conduction band at the gamma

point is formed by a triply degenerate parabolic band of heavy electrons degenerate with a nonparabolic band of light electrons.[29] The total spin degeneracy in this case would be 8; however, in our simplification we ignore the light electrons. In fact, the results are rather insensitive to the value of γ. Assuming $n_c \ll N_a$ at sufficiently low temperature, Eq. (7) can be written as

$$n_c = \frac{N_c}{\gamma}\left(\frac{N_d - N_a}{N_a}\right)\exp\left(-\frac{E_d}{k_B T}\right). \tag{8}$$

Then, the Hall coefficient and electrical conductivity are[30]

$$R_H = \frac{n_c \mu_c^2 + n_i \mu_i^2}{e(n_c \mu_c + n_i \mu_i)^2}, \tag{9}$$

$$\sigma_{\text{total}} = \sigma_c + \sigma_i = n_c e \mu_c + n_i e \mu_i, \tag{10}$$

were n_c is obtained from Eq. (8), and $n_i = N_d - N_a - n_c$. The peak in R_H roughly corresponds to the case where $\sigma_c \sim \sigma_i$. For temperatures below the peak, impurity conduction is the dominant transport mechanism. The band and impurity mobilities can be expressed as

$$\mu_c = A T^{-3/2}, \tag{11}$$

$$\mu_i = B \exp\left[-\frac{E_i}{k_B T}\right], \tag{12}$$

where A, B, and E_i are constants. The form of the conduction-band mobility follows from the assumption of the dominance of acoustic phonon scattering. The particular form of Eq. (12) was chosen to approximate the observed low temperature dependence of the resistivity (n_i is nearly constant at low temperatures) and is not critical to the qualitative behavior since the essential feature of this model is that $\mu_c \gg \mu_i$ for all temperatures.

A simultaneous fit of the Hall and resistivity data to Eqs. (9) and (10) was carried out and the results are shown as dashed lines in Fig. 8. The fitting parameters are given in Table I and several derived quantities are shown in Table II. Clearly, the model describes well both the large variations with temperature of the data as well as the overall trends as Ni content increases. Semiquantitative agreement of the data with the essential physics of the model are seen. First, the calculated values of N_d are within an order of magnitude of the nominal concentrations of Ni atoms, N_{Ni} in $Co_{1-x}Ni_xSb_3$—we do not expect much better agreement from this analysis. Therefore, we attribute the donor states directly to the presence of Ni substituting for Co. Second, we

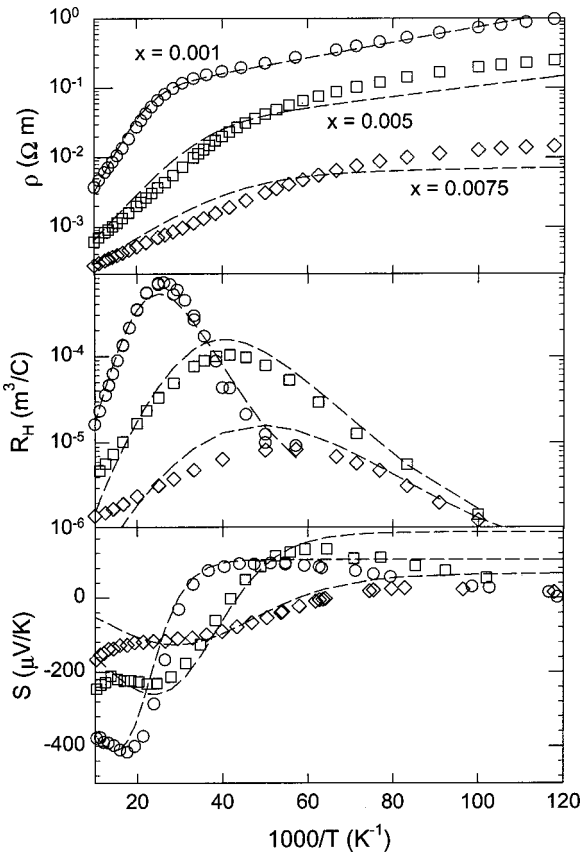

FIG. 8. Temperature dependence of electrical resistivity ρ, Hall coefficient R_H, and thermopower S for $x = 0.001$, 0.005, and 0.0075 samples. The dashed lines are fits to Eqs. (9), (10), and (13). Fitting parameters for the Hall and resistivity data are given in Table II, and for thermopower are $N_i = 2\times10^{19}$, 5×10^{19}, and 3×10^{19} cm^{-3} for $x = 0.001$, 0.005, and 0.0075, respectively.

note that $N_{\text{Ni}}^{1/3} a_B$ (as in Table II) is less than the value of $N_{\text{cri}}^{1/3} a_B \sim 0.26$ (Mott criterion[31,32]) where N_{cri} is the critical concentration and thus our samples are on the insulating side of the metal-insulator transition. For donor concentrations near the insulating side of the Mott transition, it is known that ε_1 scales as $N_d^{-1/3}$, which is observed. Third, the fact that μ_c/μ_i (Table II) decreases as N_d increases is consistent with the magnitude of the density of states in the impurity "band" increasing with N_d. These observations lend support to the model.

It is seen that the peak in R_H (the crossover from predominantly conduction band to impurity conduction) approximately matches the region where $S = 0$. This sign rever-

TABLE I. Fitting parameters of the two-band analysis of the electrical transport for $Co_{1-x}Ni_xSb_3$.

x	A ($m^2K^{3/2}/Vs$)	B (m^2/Vs)	N_d (10^{19} cm^{-3})	N_a (10^{18} cm^{-3})	E_d (meV)	E_i (meV)
0.001	7.1×10^{-5}	5.39	0.3	1.4	24.2	0.0022
0.003	4.1×10^{-5}	2.45	0.4	0.7	18.3	0.0017
0.005	5.3×10^{-5}	2.42	0.8	1.4	13.8	0.0015
0.0075	8.2×10^{-5}	1.09	1.6	0.2	8.3	0.0002

TABLE II. Nominal concentrations of Ni impurity, N_{Ni}, a comparison to the Mott criterion, $N_{\mathrm{Ni}}^{1/3} a_B$, calculated effective masses, m_n, the ratio of band to impurity mobility at 30 K, μ_c/μ_i, and compensation ratio K for $Co_{1-x}Ni_xSb_3$.

x	N_{Ni} (10^{19} cm^{-3})	$N_{\mathrm{Ni}}^{1/3} a_B$	m_n (m_0)	μ_c/μ_i ($T=30$ K)	$K=N_a/N_d$
0.001	1.1	0.11	3.60	1100	0.48
0.003	3.3	0.17	3.35	710	0.19
0.005	5.4	0.22	3.07	500	0.18
0.0075	8.1	0.20	3.92	90	0.11
0.01	10.8	0.23	3.76		

sal in S is convincing evidence of impurity conduction, and has been observed, e.g., by Geballe and Hull in Si (Ref. 33) and recently in GaN.[34] Table II shows that the compensation ratios $K=N_a/N_d$ for the samples are less than 0.5, which should give rise to impurity conduction with p-type character.[35] The total thermopower in terms of the contribution from the conduction band S_c[36] and the impurity states S_i[36] is

$$S=\frac{S_c\sigma_c+S_i\sigma_i}{\sigma_c+\sigma_i}, \tag{13}$$

$$S_{c,i}=\mp\frac{k_B}{e}\left[\delta_{c,i}+\ln\left(\frac{N_{c,i}}{n_{c,i}}\right)\right], \tag{14}$$

where $\delta_{c,i}$ is a term connected with the kinetic energy of the charge carriers, $N_{c,i}$ is the density of states in the conduction band (N_c) and impurity states (N_i), and we take ($-$) for S_c and ($+$) for S_i. We set both δ_c and δ_i to zero, approximating narrow band transport. N_c is defined above and has a $T^{3/2}$ dependence, so S_c depends only on the physical quantities derived from R_H and ρ. The thermopower of the impurity conduction is much harder to model, though the primary aspect of this term is that it is positive. As an approximation, we take N_i to be constant, and use it as an adjustable parameter in a fit to the data for $Co_{1-x}Ni_xSb_3$ with $0.001\leqslant x\leqslant 0.0075$. The values used in the fit are given in the caption to Fig. 8 and are of the same order of magnitude as N_{Ni}. The transition temperature where S changes sign should scale roughly with the depth of the donor band, ε_1, which is what we observe. A good fit is obtained employing this model in this temperature region, further strengthening the two-band picture.

Transverse magnetoresistance for $Co_{0.999}Ni_{0.001}Sb_3$ as a function of magnetic-field strength at several temperatures is shown in Fig. 9. Below 30 K, the magnetoresistance is negative. This is a common feature in doped semiconductors near the metal-insulator transition.[37,38] The electrons in the impurity "band" should be scattered on "localized spins" of partly isolated impurity atoms.[39] In the presence of a magnetic field, the spins become aligned and the scattering decreases, thereby reducing the resistance. Above 30 K, the magnetoresistance is positive and depends quadratically on the magnetic field as is expected from the deflection of the electrons residing in an ordinary band via the Lorentz force.

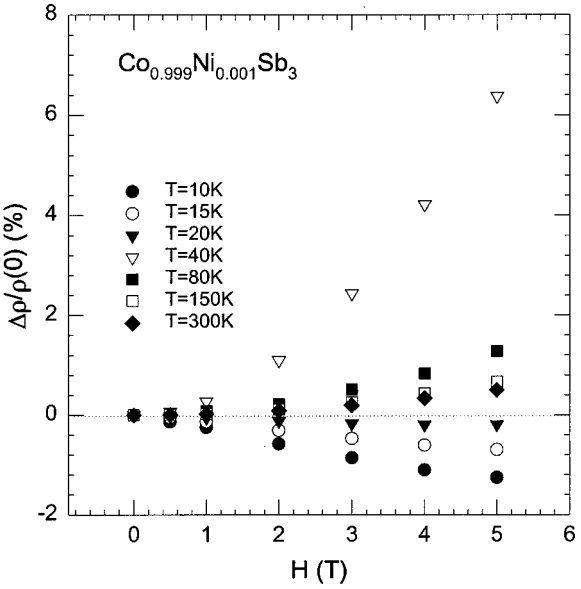

FIG. 9. Magnetic-field dependence of the transverse magnetoresistance $\Delta\rho(B)/\rho(0)$ at several temperatures for the $Co_{0.999}Ni_{0.001}Sb_3$ sample.

The peak near 40 K can be understood by taking into account the temperature dependence of the mobility of both the conduction and impurity electrons. The same effect was seen in impurity bands in GaAs.[30]

C. Magnetic Susceptibility

The magnetic moment M varies linearly with the magnetic field H at all temperatures and for all six samples measured. For $CoSb_3$, we found a diamagnetic susceptibility with a weak temperature dependence. The bonding configuration that takes into account its transport and magnetic characteristics was first postulated by Dudkin.[40] Three of the nine Co (d^7s^2) electrons bond with the Sb atoms while the remaining six nonbonding electrons adopt the maximum spin-pairing configuration, the zero-spin d^6 state. It is clear that Ni, with one more electron than Co, can reside either in the low-spin d^7 state ($s=1/2$) as a neutral impurity, or zero spin d^6 state ($s=0$) plus donor electron ($s=1/2$). Anno[20] reported an effective magnetic moment per Ni atom of about $1.7\mu_B$ (Bohr magneton) from a fit of the magnetic susceptibility to a Curie-Weiss form for $Co_{1-x}Ni_xSb_3$ with $x>0.03$ and concluded that Ni assumes the low-spin d^7 configuration. Like Anno, we obtain an effective magnetic moment per Ni atom of approximately $1.7\mu_B$ as well (see below). If this were to imply a single unpaired spin, i.e., a d^7 state, the Ni could not donate an electron to the conduction band contrary to the Ni-doping effect observed in the transport data.

To provide a consistent explanation of both transport and magnetic properties of the Ni-doped $CoSb_3$, we analyze the magnetic susceptibility χ in the context of a doped semiconductor. The transport data suggests that Ni provides an electron for transport at elevated temperatures and retains the electron at low temperatures. In this case,[41]

$$\chi(T)=\chi_i+\frac{n_i V\mu_B^2}{k_B T}+\mu_B^2 V\frac{\partial n_c}{\partial \eta}\left[\frac{g^2}{4}-\frac{1}{3}\left(\frac{m_0}{m_n}\right)^2\right], \quad (15)$$

where χ_i is the temperature-independent diamagnetic contribution from the ion cores, V is the sample volume, and g is the Landé factor for electrons. The second term arises from the unpaired spins of electrons localized at the donor impurities, and the third term is the Pauli paramagnetic and Landau diamagnetic susceptibilities of the free band electrons. In this formulation, we ignore the small diamagnetic contribution from the localized electrons and the effects due to interactions of their local moments. Because of the heavy conduction band of $CoSb_3$ (about $3m_0$), $g^2/4-1/3(m_0/m_n)^2 \cong 1$ if we let $g=2$. Furthermore, Boltzmann statistics apply at all temperatures up to room temperature for these low carrier concentrations, in which case $\partial n_c/\partial\eta \cong n_c/k_B T$. As a result, Eq. (15) becomes

$$\chi(T)=\chi_i+(n_c+n_i)\frac{V\mu_B^2}{k_B T}, \quad (16)$$

where $(n_i+n_c)=N_d$ is a constant. Therefore, the paramagnetic susceptibility of the conduction electrons at high temperature is the same as that of the localized impurity electrons at low temperature. This can explain the Curie-like behavior. In reality, there may be some magnetic correlations that result in small deviations from a purely Curie temperature dependence. In Fig. 10, we show a fit of the magnetic susceptibilities of Ni-doped samples using the Curie-Weiss form,

$$\chi-\chi_{\text{pure}}=\chi_0+\frac{C}{T+\theta_{\text{cw}}}, \quad (17)$$

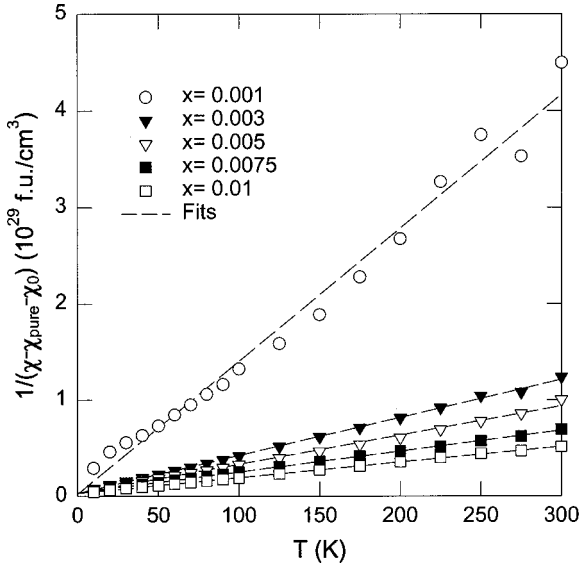

FIG. 10. $1/(\chi-\chi_{\text{pure}}-\chi_0)$ versus temperature for all $Co_{1-x}Ni_xSb_3$ samples. Dashed lines are fits according to Eq. (17).

TABLE III. The fitting parameters and the effective Bohr magneton numbers $P(\mu_B/\text{Ni})$ per nickel atom for the magnetic susceptibilities of $Co_{1-x}Ni_xSb_3$.

x	χ_0 (10^{-30} cm^3/f.u.)	C (10^{-28} cm^3-K/f.u.)	θ_{cw} (K)	P (μ_B/Ni)
0.001	7.766	8.526	15.58	2.027
0.003	−0.875	26.45	11.17	2.062
0.005	−2.388	35.23	15.99	1.843
0.0075	−1.978	46.70	17.32	1.733
0.01	−1.361	62.43	19.85	1.735

where χ_{pure} is the magnetic susceptibility of the undoped sample, χ_0 is a small temperature-independent term reflecting the difference of the ionic core contribution between the pure and Ni-doped samples, C is the Curie constant, and θ_{cw} is the Curie-Weiss temperature. Table III lists the fitting parameters.

Our magnetic data suggests that the magnetic susceptibility, unlike the electron transport data, is not sensitive to whether the electrons are in the impurity states or the conduction band. Instead of a core d^7 state as proposed by Anno, we believe the core electrons of Ni preserve the zero-spin d^6 configuration and the Ni^{4+} state makes available a conduction electron for transport. At low T, this conduction electron is recaptured by the Ni impurity as a localized spin with $s=1/2$, consistent with the $1.7\mu_B$ magnetic moment we observe. At high T, this electron becomes delocalized, and gives rise to "band" paramagnetism. We thus conclude that Ni takes the tetravalent state Ni^{4+}, i.e., the zero-spin d^6 electronic configuration. We, therefore, have a consistent picture for both the transport and magnetic susceptibility of $Co_{1-x}Ni_xSb_3$ consisting of electrons residing in the conduction band and impurity states. A more sensitive test of the valence state of Ni, e.g., electron paramagnetic resonance, would be very revealing in confirming our picture.

V. SUMMARY

We performed transport and magnetic measurements on a series of polycrystalline samples of the form $Co_{1-x}Ni_xSb_3$ with $x=0$, 0.001, 0.003, 0.005, 0.0075, and 0.01. Such minute amount of impurity is sufficient to change the transport from p type to n type. Ni doping dramatically changes the temperature dependence of the thermopower. A very high thermopower ($S\sim 500\ \mu$V/K) is achieved for $x=0.001$. At low temperatures, very sharp peaks in the Hall coefficient are observed to correlate with anomalous features in thermopower. A two-band model consisting of the conduction band and an impurity "band" formed by the Ni impurities accounts for the observed behavior. The magnetic susceptibility is also analyzed within the picture of donor (localized) and band (itinerant) electrons, thereby resolving the seemingly inconsistent Curie-Weiss-like behavior that suggests the Ni atoms are trivalent, making it difficult to account for the clear doping effect Ni has on $CoSb_3$. Our magnetometry and transport data indicate that Ni takes the tetravalent state

Ni^{4+}, assuming the d^6 electronic configuration for the lower-energy nonbonding orbitals, and gives one electron to the conduction band. These results show that Ni acts as a donor and may prove useful for optimizing the carrier concentration in optimally filled skutterudite materials.

ACKNOWLEDGMENTS

We thank Dr. D. T. Morelli for helpful discussions. This work is supported in part by DARPA under Contract No. 00014-98-3-0011.

[1] C. Uher, in *Semiconductors and Semimetals*, Vol. 69, edited by T. M. Tritt (Academic Press, San Diego, CA, 2000), p. 139.
[2] G. S. Nolas, D. T. Morelli, and T. M. Tritt, Annu. Rev. Mater. Sci. **29**, 89 (1999).
[3] W. Jeitschko and D. J. Brown, Acta Crystallogr. **B33**, 3401 (1977).
[4] N. T. Stetson, S. M. Kauzlarich, and H. Hope, J. Solid State Chem. **91**, 140 (1994).
[5] B. C. Sales, B. C. Chakoumakos, and D. Mandrus, Phys. Rev. B **61**, 2475 (2000).
[6] G. P. Meisner, D. T. Morelli, S. Hu, J. Yang, and C. Uher, Phys. Rev. Lett. **80**, 3551 (1998).
[7] J. Yang, G. P. Meisner, D. T. Morelli, and C. Uher, Phys. Rev. B **63**, 014410 (2001).
[8] D. T. Morelli, T. Caillat, J.-P. Fleurial, A. Borshchevsky, J. Vandersande, B. Chen, and C. Uher, Phys. Rev. B **51**, 9622 (1995).
[9] J. W. Sharp, E. C. Jones, R. K. Williams, P. M. Martin, and B. C. Sales, J. Appl. Phys. **78**, 1013 (1995).
[10] T. Caillat, A. Borshchevsky, and J.-P. Fleurial, J. Appl. Phys. **80**, 4442 (1996).
[11] D. Mandrus, A. Migliori, T. W. Darling, M. F. Hundley, E. J. Peterson, and J. D. Thompson, Phys. Rev. B **52**, 4926 (1995).
[12] E. Arushanov, K. Fess, W. Kaefer, Ch. Kloc, and E. Bucher, Phys. Rev. B **56**, 1911 (1997).
[13] H. Anno, K. Hatada, H. Shimizu, K. Matsubara, Y. Notohara, T. Sakakibara, H. Tashiro, and K. Motoya, J. Appl. Phys. **83**, 5270 (1998).
[14] L. D. Dudkin and N. Kh. Abrikosov, Zh. Neorg. Khim. **2**, 212 (1957).
[15] B. N. Zobrina and L. D. Dudkin, Sov. Phys. Solid State **1**, 1668 (1960).
[16] J. Yang, D. T. Morelli, G. P. Meisner, and C. Uher, in *Thermal Conductivity 25/Thermal Expansion 13*, edited by C. Uher and D. T. Morelli (Technomic Publishing, Lancaster, PA, 2000), p . 130.
[17] S. Katsuyama, Y. Shichijo, M. Ito, K. Majima, and H. Nagai, J. Appl. Phys. **84**, 6708 (1998).
[18] K. L. Stokes, A. C. Ehrlich, and G. S. Nolas, in *Thermoelectric Materials 1998—The Next Generation Materials for Small-Scale Refrigeration and Power Generation Applications*, edited by T. M. Tritt and H. B. Lyon, Jr., Mater. Res. Soc. Symp. Proc. No. **545** (Materials Research Society, Pittsburgh, 1999).
[19] H. Anno, K. Matsubara, Y. Notohara, T. Sakakibara, and H. Tashiro, J. Appl. Phys. **86**, 3780 (1999).
[20] H. Anno, H. Tashiro, and K. Matsubara, *Proceedings of the 18th International Conference on Thermoelectrics, Baltimore, 1999*, IEEE Catalog No. 99TH840 (IEEE, Piscataway, NJ, 1999), p. 169.
[21] C. Uher, J. Appl. Phys. **62**, 4636 (1987).
[22] B. Chen, J. Xu, C. Uher, D. T. Morelli, G. P. Meisner, J.-P. Fleurial, T. Caillat, and A. Borshchevsky, Phys. Rev. B **55**, 1476 (1997).
[23] J. Y. W. Seto, J. Appl. Phys. **46**, 5247 (1975).
[24] H. J. Goldsmid, *Electronic Refrigeration* (Pion Limited, London, 1986).
[25] D. J. Singh and W. E. Pickett, Phys. Rev. B **50**, 11 235 (1994).
[26] J. O. Sofo and G. D. Mahan (Ref. 18).
[27] N. F. Mott, J. Non-Cryst. Solids **1**, 1 (1968).
[28] G. Kliche and H. D. Lutz, Infrared Phys. **24**, 171 (1984).
[29] J. O. Sofo and G. D. Mahan, Phys. Rev. B **58**, 15 620 (1998).
[30] O. V. Emel'yanenko, T. S. Lagunova, D. N. Nasledov, and G. N. Talalakin, Fiz. Tverd. Tela **7**, 1315 (1965) [Sov. Phys. Solid State **7**, 1063 (1965)].
[31] N. F. Mott, Proc. Cambridge Philos. Soc. **32**, 281 (1949).
[32] P. P. Edwards and M. J. Siendo, Phys. Rev. B **17**, 2575 (1978).
[33] T. H. Geballe and G. W. Hull, Phys. Rev. **98**, 940 (1955).
[34] M. S. Brandt, P. Herbst, H. Angerer, O. Ambacher, and M. Stutzmann, Phys. Rev. B **58**, 7786 (1998).
[35] N. F. Mott and E. A. Davis, *Electronic Processes in Non-Crystalline Materials*, 2nd ed. (Clarendon, Oxford, 1979).
[36] A. F. Ioffe, *Physics of Semiconductors* (Infosearch Limited, London, 1960).
[37] Y. Katayama and S. Tanaka, Phys. Rev. **153**, 873 (1967).
[38] L. Halbo and R. J. Sladek, Phys. Rev. **173**, 794 (1968).
[39] Y. Toyozawa, J. Phys. Soc. Jpn. **17**, 986 (1962).
[40] L. D. Dudkin, Fiz. Tverd. Tela **2**, 397 (1960) [Sov. Phys. Solid State **2**, 371 (1960)].
[41] S. V. Vonsovskii, *Magnetism* (Wiley, New York, 1974), p. 264.